Matching oceanography and genetics at the basin scale. Seascape connectivity of the Mediterranean shore crab in the Adriatic Sea

M. SCHIAVINA,*†[1] I. A. M. MARINO,‡[1] L. ZANE†‡ and P. MELIÀ*†
*Dipartimento di Elettronica, Informazione e Bioingegneria, Politecnico di Milano, via Ponzio 34/5, I-20133 Milano, Italy, †Consorzio Interuniversitario per le Scienze del Mare, Piazzale Flaminio 9, I-00196 Roma, Italy, ‡Dipartimento di Biologia, Università di Padova, via U. Bassi 58/B, I-35131 Padova, Italy

[1]Equally contributed to the study.

Received 18 July 2014; revision received 25 September 2014; accepted 3 October 2014

Introduction

Seascape connectivity, the process linking habitat patches and populations through the exchange of organisms across the marine environment, is a key driver of population dynamics and genetic structuring, and is therefore central to defining management and conservation units (White *et al.* 2010). For many marine organisms, connectivity is essentially determined by larval dispersal (Ward *et al.* 1994). Larvae, however, are difficult to track, due to their small size and to the rapid dilution of larval density with distance and time from the natal origin (Cowen & Sponaugle 2009).

Genetic methods provide an indirect measure of connectivity (Palumbi 2003). Several studies have shown that marine populations can be less connected than expected on the basis of their larval duration and absence of obvious barriers to dispersal, indicating that significant genetic differences can arise even at small spatial scales (Knowlton 2000; Swearer *et al.* 2002; Taylor & Hellberg 2003; Bilodeau *et al.* 2005; Galarza *et al.* 2009). Limited connectivity may be due to life history, larval behaviour and/or oceanographic features leading to the retention of offspring near reproductive locations (Dawson 2001; Sherman *et al.* 2008; Morgan *et al.* 2009). Inferences on population connectivity from

Correspondence: Lorenzo Zane, Fax: +390498276209;
E-mail: lorenzo.zane@unipd.it

genetic data can be effective to identify major biogeographical or oceanographic barriers (Planes 2002; Schunter *et al.* 2011), but can be problematic when differentiation is weak (Waples 1998). In this case, the major challenge is to discriminate between heterogeneity caused by stochastic factors linked to reproduction and recruitment, and true, although subtle, population genetic structure.

Coupled physical–biological models (CPBMs) can enhance the predictive value of population genetics (Gilg & Hilbish 2003; Hohenlohe 2004; Kenchington *et al.* 2006; Dupont *et al.* 2007), providing the basis for a mechanistic understanding of the links between oceanography, ecology and genetic structure (Selkoe *et al.* 2010). CPBMs are increasingly used to investigate larval dispersal and to contrast alternative hypotheses by simulation (Gallego *et al.* 2007). Validating models against experimental data is crucial to verify the reliability of simulated dispersal patterns (Hannah 2007; Melià *et al.* 2013). In this sense, a cross-validation between CPBM outputs and genetic data can be effective for verifying model predictions (Galindo *et al.* 2006, 2010) and increasing confidence on genetic analyses (Selkoe *et al.* 2010; White *et al.* 2010). When fed with data on specific vital traits affecting dispersal, CPBMs are particularly useful to investigate the effects of temporal variation in ocean currents on potential dispersal. Very different patterns of gene flow can emerge simply from different matching between reproductive timing and seasonal current patterns (Carson *et al.* 2010). CPBMs and genetic data have been used to investigate geneflow direction in the comber *Serranus cabrilla* across the major oceanographic discontinuities of the western Mediterranean (Schunter *et al.* 2011). A similar approach has been used for the white sea bream (*Diplodus sargus*) in the central Mediterranean, to demonstrate panmixia between marine protected areas and neighbouring nonprotected areas (Di Franco *et al.* 2012; Pujolar *et al.* 2013).

In this work, we investigate connectivity patterns of the Mediterranean shore crab *Carcinus aestuarii* in the Adriatic Sea, by coupling Lagrangian simulations that integrate key vital traits and genetic microsatellite analyses of population samples covering 1200 km of the Italian coastline. *Carcinus aestuarii* is a highly dispersive species inhabiting lagoons and estuaries, whose females release larvae in the adjacent coastal waters after a very short migration towards the open sea (Mori *et al.* 1990). A previous study, based on mitochondrial cytochrome c oxidase I sequencing, did not detect differences among Adriatic population samples, which, in contrast, differed significantly from those collected in the western Mediterranean and Tyrrhenian seas (Marino *et al.* 2011). Another study, using microsatellites, pointed out the existence of genetic patchiness among population samples from the northern Adriatic Sea, in a context lacking any geographic differentiation over a scale of about 200 kilometres (Marino *et al.* 2010).

Here, we extend the microsatellite analysis to the scale of the whole Adriatic basin and integrate it with CPBM simulations, with the aim of understanding how currents shape the genetic structure of *C. aestuarii* by mediating larval dispersal. The surface circulation of the Adriatic Sea is characterized by a large-scale cyclonic meander, with a northerly flow along the eastern coast and a southerly flow along the western coast (Orlić *et al.* 1992). Within this large system, three cyclonic gyres subdivide the basin into three regions, with a northern gyre defined mainly in autumn at the surface, a middle gyre and a southern gyre that become more intense in summer and autumn (Artegiani *et al.* 1997). Circulation patterns are affected by remarkable seasonal and short-term variation. The existence of three main gyral systems provides a working hypothesis for investigating the genetic subdivision of *C. aestuarii* populations, and CPBMs are expected to provide insights on the interactions between life history schedule and current seasonality.

Specifically, we aim to (i) identify the presence of genetic structure among Adriatic population samples and compare them with those from the Ionian and Tyrrhenian seas; (ii) compare different scenarios of gene flow, including models with negligible exchange between populations and models with directional migration; (iii) estimate potential larval connectivity and retention via a CPBM incorporating vital traits affecting larval dispersal; and (iv) contrast genetic data and modelling results to understand the consequences of water circulation on the genetic structure of *C. aestuarii*.

Materials and methods

Sampling

Four hundred and thirty-one samples of *Carcinus aestuarii* were collected from 2006 to 2008 at eight different sites (Fig. 1, Table 1). Six sites were located in the Adriatic Sea, and two additional sites in the Ionian and Tyrrhenian seas were included for comparison. At each location, about 50 adult crabs were caught with baited hoop nets. After collection, crabs were brought to the laboratory and muscle tissue was removed from one cheliped and frozen at −80 °C until DNA extraction.

DNA extraction and microsatellite genotyping

Total genomic DNA was extracted using a salting-out protocol (Patwary *et al.* 1994). Eight polymorphic micro-

satellite loci specific for *C. aestuarii* (Cae01, Cae07, Cae14, Cae17, Cae30, Cae33, Cae71, Cae86; Marino *et al.* 2008) and three additional microsatellite loci originally isolated from the sibling species *C. maenas* (Cma02EPA, Cma04EPA, Cma14EPA; Tepolt *et al.* 2006) were used for genetic analysis. Information on microsatellite features and amplification conditions are reported in Marino *et al.* (2010). Fragment analysis was performed by an external service (http://www.bmr-genomics.it) on an ABI 3100 automated sequencer, and PCR products were sized with the internal standard GS 400 Hd Rox (Applied Biosystems). To ensure reproducibility of results and minimize differences due to capillary electrophoresis, 10–15% of all specimens was regenotyped and rescored. Scoring was performed with GENOTYPER 3.7 (Applied Biosystems). To minimize the negative consequences of poor allele calling, binning was automated with FLEXIBIN 2 (Amos *et al.* 2007). The scoring was manually checked and analysed for the presence of null alleles with MICROCHECKER 2.2.3 (Van Oosterhout *et al.* 2004).

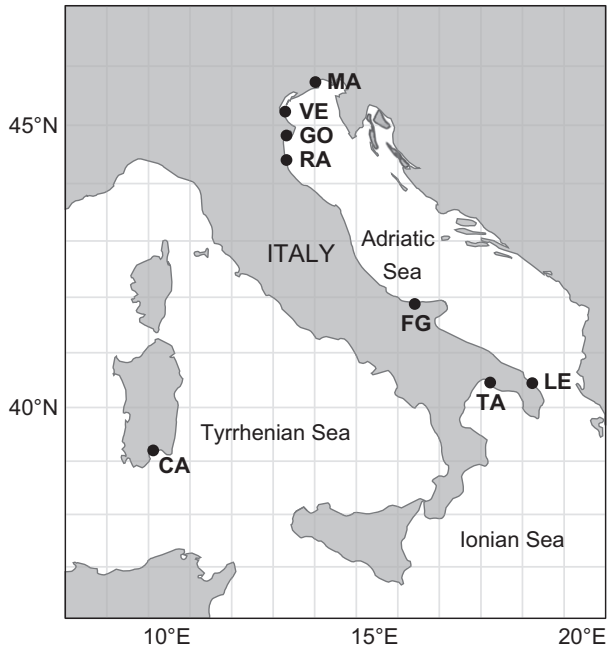

Fig. 1 Sampling locations of *Carcinus aestuarii*. See Table 1 for location codes.

Genetic diversity, Hardy–Weinberg and linkage equilibrium, and power analysis

Number of alleles (N_A), observed (H_O) and unbiased expected (H_E) heterozygosity, departure from Hardy–Weinberg equilibrium (HWE) per locus and site, and linkage equilibrium per locus were calculated with GENEPOP 3.4 (Raymond & Rousset 1995; Rousset 2008). Significance levels of HWE and linkage equilibrium were determined via the Markov Chain method (dememorizations = 10000, batches = 500, iterations = 10000); significance for tests involving multiple comparisons was obtained using the SGOF+ software (Carvajal-Rodriguez & de Uña-Alvarez 2011). Allelic richness (A_R) was computed with FSTAT 2.9.3.2 (Goudet 2001) based on the smallest sample size across all population samples.

Statistical power for detecting genetic differentiation was estimated with POWSIM 4.1 (Ryman & Palm 2006), which mimics sampling from populations at various levels of expected divergence under a classical Wright–Fisher drift model without migration or mutation. The power to detect an expected divergence as small as $F_{ST} = 0.001$ was tested by running 1000 simulations, each consisting of six generations of drift (t). Effective population size was set to 3000, and allele frequencies from the current data set were used as a starting point. At the end of each simulation, genotypic samples with

Table 1 *Carcinus aestuarii* population samples used in this study

Location	Code	Basin	Geographic coordinates		Sampling year	Sample size
			East	North		
Marano	MA	North Adriatic Sea	13.137	45.728	2006	55
Venice	VE	North Adriatic Sea	12.290	45.236	2006	47
Goro	GO	North Adriatic Sea	12.316	44.830	2006	60
Ravenna	RA	North Adriatic Sea	12.316	44.413	2007	50
Lesina	FG	Central Adriatic Sea	15.407	41.883	2008	54
Acquatina	LE	South Adriatic Sea	18.238	40.442	2007	67
Taranto	TA	Ionian Sea	17.218	40.457	2008	48
Cagliari	CA	Tyrrhenian Sea	9.113	39.204	2007	50
Total						431

Samples are arranged from north to south. Geographic coordinates are expressed in decimal degrees.

number and sizes corresponding to those of the empirical data set were collected and statistical testing of homogeneity performed. The proportion of significant outcomes ($P < 0.05$) among replicates represents the estimate of power.

Bayesian clustering analysis

We investigated the spatial genetic structure with two different Bayesian clustering methods. First, STRUCTURE 2.3.3 (Pritchard *et al.* 2000; Falush *et al.* 2003, 2007; Hubisz *et al.* 2009) was used to estimate the most likely number of populations represented by the samples. STRUCTURE is a model-based Bayesian, Markov chain Monte Carlo approach that clusters individuals to minimize Hardy–Weinberg disequilibrium and gametic phase disequilibrium between loci within groups. The Bayesian model assumes K (unknown) populations with different allele frequencies at a set of independent loci. The program was run with 20 independent simulations for each value of K from 1 to 5, each with 1 000 000 iterations, following a burn-in period of 100 000 iterations. We used the LOCPRIOR model (Hubisz *et al.* 2009) that utilizes sampling locations as prior information to assist the clustering and is appropriate when the signal of structure is relatively weak. In all simulations, individual admixture proportions (q) and their 95% posterior probability intervals were calculated by assuming an admixture ancestry model (i.e. allowing the genetic composition of individuals to be a mixture from different populations) and a correlated allele frequencies model ($\lambda = 1$). The ΔK statistic of Evanno *et al.* (2005) was used to infer the most likely number of real populations and was calculated with STRUCTURE HARVESTER (Earl & vonHoldt 2012).

Then, we refined the analysis with GENELAND 3.2.4 (Guillot *et al.* 2005) in the R-PACKAGE 2.11.1 (R Development Core Team 2010). By incorporating geographical data as a weak prior into the clustering procedure, GENELAND is able to detect subtle population structure, as well as to infer the probable location of genetic transition zones (Guillot *et al.* 2005; Jones *et al.* 2010). To determine the number of genetic clusters, 10 independent runs were performed using 1 000 000 MCMC iterations with a burn-in period of 100 000, a thinning value of 100 and a maximum rate of the Poisson process set to 100. The minimum K was set to 1 and the maximum to 5. We used the correlated frequency model to allow detection of subtle structures in the presence of low genetic differentiation that would probably remain undetected using an uncorrelated frequencies model (Guillot 2008). In this case, we excluded from the analysis the geographically distant sample from Cagliari (CA) with the aim of improving the definition of the spatial genetic units at the local scale. Results of GENELAND clustering were confirmed using nonlinear MultiDimensional Scaling (nMDS), with STATISTICA 10 (STATSOFT); Reynolds coancestry coefficients (Reynolds *et al.* 1983) were used as distance measure.

Population differentiation and gene flow

Overall levels of genetic differentiation were calculated by $F_{ST,}$ estimated by f (Weir & Cockerham 1984) using FSTAT. The significance of F_{ST} was tested on the basis of a random permutation procedure with ARLEQUIN 3.5 (Excoffier & Lischer 2010). Pairwise F_{ST} were determined with GENETIX (Belkir *et al.* 2005), using 10 000 permutations for all comparisons among population samples; as before, SGOF+ correction for multiple tests was applied. Genetic divergence among groups of populations was analysed also using hierarchical analysis of molecular variance (AMOVA; Excoffier *et al.* 1992; Excoffier & Lischer 2010).

Isolation by distance (IBD) was assessed by plotting pairwise $F_{ST}/(1 - F_{ST})$ values (Rousset 1997) against geographic distance (measured as the distance along the coast, in km) for all pairwise comparisons between sites. A Mantel test (10 000 permutations) was conducted to estimate the significance and strength of the relationship between genetic and geographic distances with ARLEQUIN 3.5 (Excoffier & Lischer 2010).

Population genetics was further investigated with the Bayesian coalescent approach implemented in MIGRATE-n 3.6.4 (Beerli & Palczewski 2010). Given the low genetic differentiation, the software was used to compare alternative models of gene flow rather than estimating connectivity directly, and the analysis was conducted on data pooled to represent the groups identified by GENELAND. Four geneflow models were compared using Bayes factors: a model assuming negligible connection among sites, obtained by setting migration probabilities to values close to zero (describing a scenario in which weak differences between samples reflect a recent common ancestry rather than high levels of gene flow), a full model with distinct populations and independent migration rates, and two models with migration occurring only from north to south or vice-versa.

MIGRATE-n was run using a Bayesian model and, as starting values, the estimates obtained from previous runs, with the following parameters: microsatellites Brownian model (Beerli & Felsenstein 2001), uniform priors for θ (mutation-scaled effective population size) ranging between 0 and 250, and for M (ratio of immigration rate to mutation rate) ranging between 0 and 1000. A static heating scheme with four chains and temperatures set at 1–1.5–3–10 000, ordered from cold to boiling, was used; chains were run with 100 sampling increment, 10 000 recorded steps and 100 000 discarded

trees per chain (burn-in). Convergence was checked by inspecting posterior distributions of the parameters and comparing results of two replicated runs. Log marginal likelihoods of the different runs were compared using Bezier approximation (Beerli & Palczewski 2010), and log Bayes factors (LBF) were calculated, following the guidelines in Kass & Raftery (1995). In addition, model probabilities were calculated by dividing each marginal likelihood by the sum of the marginal likelihoods of all the models according to MIGRATE-n tutorial.

Lagrangian simulations

Lagrangian simulations were based on daily average fields of current velocity and water temperature produced by the Adriatic Forecasting System (http://oceanlab.cmcc.it/afs/). The data set is generated by the Adriatic Sea Regional Model (Oddo *et al.* 2006; Guarnieri *et al.* 2010), covering the whole Adriatic basin and extending south of the Otranto channel into the Ionian Sea down to the 39°N parallel. The model has a regular horizontal grid with a resolution of 1/45° (about 2.2 km) and 31 vertical sigma layers. Model bathymetry has a horizontal resolution of 1/60°, with the coastline set at the 10-m isobath.

Lagrangian particles were released from each of the seven Adriatic and Ionian sites at which genetic samples had been collected and where reproduction occurs. Releases were distributed throughout the period in which sampled individuals were likely born: assuming an average age at capture of 3 years, simulations were started between 2003 and 2007. Releases were modulated to fit the spawning season of *C. aestuarii*, extending from September to December (as revealed by landings of egg-bearing females reported from the Chioggia fish market; Mazzoldi *et al.* 2014) and in correspondence with neap tides (Marta-Almeida *et al.* 2006). At each spawning event, 10 000 particles representing individual zoeae were released according to a 3-D Gaussian distribution in coastal waters within a 1 km radius from each site to take into account female migration towards the open sea (Mori *et al.* 1990).

Trajectories were stepped forward using a fourth-order Runge–Kutta method with a 6-minute time step and followed until the end of the pelagic phase, that is when larvae develop into megalopae and colonize estuaries and lagoons. Retention and connectivity were calculated as the percentage of larvae whose final position fell within a 5-km-radius buffer from the release or destination site, respectively. The buffer size accounts for the swimming and navigation ability of megalopae, which follow the freshwater lure and use selective tidal stream transport to reach suitable settlement areas (Queiroga 1998).

We integrated the diel vertical migration performed by zoeae (Queiroga *et al.* 1997) in our model by combining two approaches described in Marta-Almeida *et al.* (2006). We subdivided the water column into six equally spaced layers between 0 and 60 m (or down to the bottom when depth was <60 m). Every morning at 06:00, each particle was assigned to a diurnal layer, randomly determined according to the probability distribution proposed by Marta-Almeida *et al.* (2006). Then, particles were released from their current position towards the destination layer at a constant speed of 1 cm/s (Chia *et al.* 1984). Once they reached the target layer, they were allowed to move randomly within it (within a depth range of $\pm$ 0.5 m). Every evening at 18:00, particles were assigned to a nocturnal layer (according to the relevant probability distribution), allowed to migrate away from the surface (similarly to the upwards migration) and remained in the layer until next morning.

We expressed pelagic larval duration and survival as functions of water temperature through the relationships derived by deRivera *et al.* (2007) for the sibling species *C. maenas*, whose vital traits are very similar (Behrens Yamada & Hauck 2001; Klassen & Locke 2007). The duration of the zoea stage was linked to water temperature (T) through a logarithmic function $\tau = 130.46 - 36.93 \ln T$. To account for the variability of the temperature to which larvae are subject during the simulations (which would determine a different pelagic larval duration at each time step), we introduced a dummy metric D (ranging between 0 and 1) representing the development of each zoea (with $D = 0$ at birth and $D = 1$ at full development into megalopa). We expressed the progress of larval development through time as $dD/dt = \delta$, where $\delta = 1/\tau$ (with τ given by the above-cited relationship with T). By integrating D throughout the simulation, the end of the zoea stage was determined when $D = 1$. Survival (σ) over the zoea stage was expressed as a polynomial function of temperature, namely $\sigma = -0.004T^2 + 0.14T - 0.74$ (deRivera *et al.* 2007). We derived the instantaneous rate of natural mortality as $\mu = -\ln(\sigma)/\tau$ (where σ and τ are both functions of T) and were therefore able to describe the variation in μ for larvae experiencing different temperature patterns. Temperatures <6.5 °C or >28.5 °C (for which σ becomes <0) were considered to be lethal, while μ attains its lowest value (0.025/day) at an intermediate temperature of 13.9 °C.

Results

Genetic diversity, Hardy–Weinberg and linkage equilibrium, and power analysis

The analysis of 11 microsatellite loci in 431 individuals of *C. aestuarii* revealed relatively high molecular varia-

tion (Table S1, Supporting Information). PCR products from repeated amplification of the same individual consistently produced the same genotype and reliably amplified in every sample. All loci were polymorphic, with 2–39 alleles per site, and allelic richness from 2 to 35.14. Observed and expected heterozygosity ranged between 0.04–0.98 and 0.04–0.97, respectively, with a general excess of homozygotes at all loci. Overall, differences among sites were not significant for any of these statistics (one-way ANOVA, $P > 0.05$). Probability tests of Hardy–Weinberg equilibrium (HWE) were conducted for each of the 11 loci and for each of the eight sites. Thirty-one of 88 tests showed a significant departure from HWE, almost sevenfold as high as expected with a global significance threshold of 0.05. Departures were distributed almost evenly across sites and loci, although five significant tests involved two of the northern Adriatic population samples (VE and RA) and 22 significant tests involved loci Cae07, Cae33, Cma02EPA and Cma14EPA. For these loci, MICROCHECKER suggested the presence of null alleles. After correction for null alleles, all tests for HWE remained significant, suggesting that deviation was due to biological factors rather than to PCR artefacts. According to the results from HWE and MICROCHECKER, all differentiation tests were performed considering both uncorrected data and data corrected for the presence of null alleles; as this correction did not affect the final results, we report only those for uncorrected data. Overall, tests for linkage disequilibrium among all loci showed no significant departure from expected values. POWSIM results indicated that the number of loci, the number of alleles per locus, their frequency distributions and the sample sizes used were sufficient to reveal population structure at a true F_{ST} as low as 0.001 with a statistical power >85%.

Population differentiation and gene flow

The results of running STRUCTURE on the complete data set showed that genetic variation can be partitioned into two main clusters: in each run, the likelihood of K increased substantially from 1 to 2, and then levelled off or even decreased for higher values. The distribution of ΔK showed a mode at $K = 2$. The CA sample (Tyrrhenian Sea) was clearly separated from the others, which were aggregated into the second cluster. Considering the poor performance of STRUCTURE to capture further subdivisions when differentiation is low (Waples & Gaggiotti 2006), we refined the analysis with GENELAND after excluding CA. In this analysis, posterior distributions for K displayed a clear mode at $K = 3$ (Figure S1, Supporting Information), suggesting the existence of three spatially coherent clusters (Fig. 2; Figure S2, Supporting Information): the first included sites from the

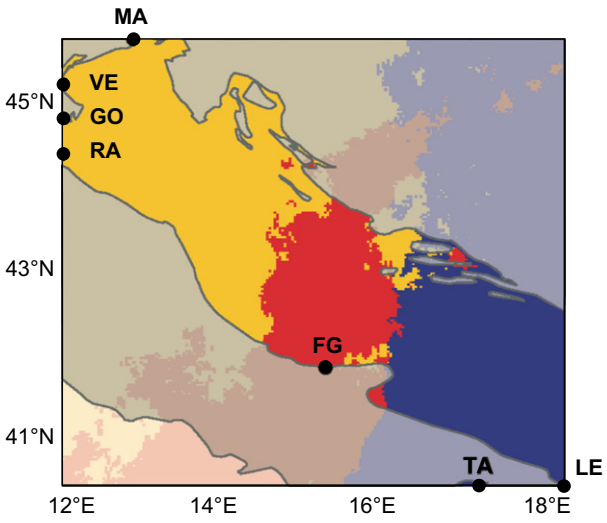

Fig. 2 Map of estimated population membership (by posterior mode) indicating northern Adriatic Sea (yellow), central Adriatic Sea (red) and southern Adriatic Sea (blue) clusters. Shaded areas indicate landmasses and the Tyrrhenian Sea, where posterior modes have no biological meaning. See Table 1 for location codes.

northern Adriatic Sea (MA, VE, GO, RA), the second the central Adriatic Sea (FG) and the third locations from the southern Adriatic and Ionian seas (LE, TA). This clustering was also supported by nMDS analysis based on Reynolds coancestry coefficients (Figure S3, Supporting Information).

The genetic differentiation detected with STRUCTURE and GENELAND Bayesian clustering analysis was further investigated using F_{ST} and AMOVA. Overall, F_{ST} was 0.009 ($P < 0.001$), indicating low but significant differentiation among locations. Pairwise F_{ST} confirmed that the largest differentiation was between the Tyrrhenian site (CA) and the other locations, with highly significant pairwise F_{ST} values ranging between 0.027 and 0.039 ($P < 0.001$, Table 2). Differentiation among the other sites was considerably lower (pairwise F_{ST} from −0.001 to 0.005), although overall panmixia was rejected for the totality of Adriatic and Ionian population samples (overall $F_{ST} = 0.002$; $P < 0.01$) and five of 21 comparisons were significant (Table 2), suggesting a certain degree of genetic structuring inside the two basins.

The partition of total genetic variance into two groups (the first including only the CA population and the second including the remaining sites), following pairwise F_{ST} and STRUCTURE results, confirmed the presence of a significant genetic structure ($F_{CT} = 0.032$, $P < 0.001$). However, a weak yet significant differentiation was found among locations within groups ($F_{SC} = 0.002$, $P < 0.05$). Hence, we tested the significance of the clustering identified by GENELAND after removing CA. A sig-

Table 2 *Carcinus aestuarii* pairwise genetic differentiation

	MA	VE	GO	RA	FG	LE	TA	CA
MA	—	0.134	0.091	0.155	**0.016**	**0.025**	**0.037**	**0.000**
VE	0.002	—	0.283	0.331	0.433	0.053	0.07	**0.000**
GO	0.002	0.001	—	0.808	0.525	0.137	0.149	**0.000**
RA	0.002	0.001	−0.001	—	0.175	0.250	0.065	**0.000**
FG	**0.004**	0.000	0.000	0.002	—	**0.035**	**0.007**	**0.000**
LE	**0.003**	0.003	0.002	0.001	**0.003**	—	0.345	**0.000**
TA	**0.003**	0.003	0.002	0.003	**0.005**	0.000	—	**0.000**
CA	**0.031**	**0.039**	**0.038**	**0.035**	**0.038**	**0.027**	**0.028**	—

Estimates of pairwise F_{ST} among eight population samples are reported below the diagonal; associated *P*-values are reported above the diagonal. Significant values after correction for multiple test, as implemented in SGOF+ (Carvajal-Rodriguez & de Uña-Alvarez 2011), are reported in bold. See Table 1 for location codes.

nificant differentiation was detected (F_{CT} = 0.002, $P < 0.01$) among the three clusters, the first one comprising MA, VE, GO and RA (northern Adriatic Sea), the second represented by FG (central Adriatic Sea) and the third containing LE and TA (southern Adriatic and Ionian seas).

The relationship between genetic and geographic distance was significant (Mantel test: $r = 0.933$, $P = 0.01$ after 10 000 permutations, Figure S4, Supporting Information) when including the Tyrrhenian location (CA). However, no significant IBD was observed ($r = 0.368$, $P = 0.06$, Figure S4, Supporting Information) when considering only the Adriatic and Ionian seas. Different scenarios of gene flow and connectivity were investigated using MIGRATE-n. Results showed a much better fit for the full model (assuming that all pairs of sites were connected) than for the one assuming negligible connection (LBF = 1.94×10^7), indicating the importance of migration in explaining the observed genetic data. The best scenario, however, was the one in which only a southward migration was assumed (probability of being the best model among all the four models tested = 0.999) that outperformed both the full model (LBF = 2.10×10^6) and the one with northward-oriented gene flow (LBF = 8.20×10^5).

Lagrangian simulations

The results of the Lagrangian simulations are summarized in Fig. 3, which shows dispersal patterns across the Adriatic and Ionian seas over the simulation period (2003–2007). Table 3 shows the estimated oceanographic connectivity (averaged over that period) among the seven locations. Retention (represented by the diagonal elements of the matrix) was low (<1%) for all locations

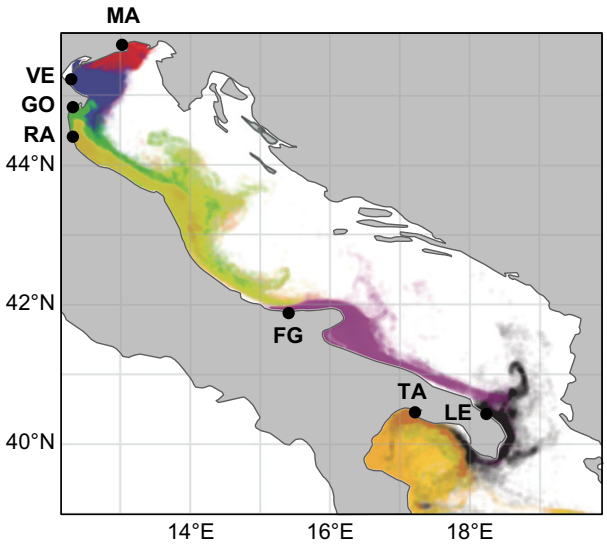

Fig. 3 Larval dispersal resulting from Lagrangian simulation. Each dot forming the coloured plumes shows the arrival location of a particle released over the time horizon of the simulation (2003–2007). Colours indicate the location of release (red: MA, blue: VE, green: GO, yellow: RA, purple: FG, black: LE, orange: TA; See Table 1 for location codes).

Table 3 *Carcinus aestuarii* connectivity

	MA (%)	VE (%)	GO (%)	RA (%)	FG (%)	LE (%)	TA (%)
MA	**0.084**	**0.011**	**0.005**	**0.003**	0.000	0.000	0.000
VE	**0.010**	**0.270**	**0.096**	**0.030**	0.000	0.000	0.000
GO	0.000	0.000	**0.110**	**0.303**	0.000	0.000	0.000
RA	0.000	0.000	**0.032**	**0.473**	**<0.001**	0.000	0.000
FG	0.000	0.000	0.000	0.000	**0.081**	**0.001**	0.000
LE	0.000	0.000	0.000	0.000	0.000	**32.710**	**0.018**
TA	0.000	0.000	0.000	0.000	0.000	0.000	**0.187**

Larval connectivity (estimated via Lagrangian simulation) indicates the percentage of larvae successfully moving from one site (rows) to another (columns) and is averaged across years and throughout the reproductive season. Values >0 are in bold. Shaded cells indicate retention. See Table 1 for location codes.

but one (LE, southern Adriatic Sea). Dispersal was predominantly oriented southwards, as can be noted from Fig. 3 and the fact that the elements above the diagonal of the connectivity matrix (Table 3) are systematically larger than the corresponding ones laying below the diagonal (which represent the flow connecting the same locations in the opposite direction). In accordance with genetic results, Lagrangian simulations pointed out connections among the four northern sites (MA, VE, GO, RA), with two pairs of sites (MA – VE, GO – RA) each connected by a bidirectional exchange of individuals. Those four sites were almost isolated from the others, except for a very low exchange of individuals (<0.001%)

from RA (northern Adriatic Sea) to FG (central Adriatic Sea). The three southernmost locations were connected by a weak flow of larvae, clearly oriented from north to south or from southern Adriatic to the Ionian Sea.

Figure 4 shows how connectivity was affected by the seasonal variation of water circulation. Retention in the northern Adriatic was highest in September and became weaker in the following months. The same holds for the site in the central area (FG), while retention in the southern site (LE) was strong and constant throughout the year. Connectivity across northern sites also changed over months, with the strength of most flows peaking between September and October. In particular, in November, the connection between GO and RA (northern Adriatic Sea) became open in both directions. On the contrary, the exchange of individuals across southern locations was more intense in late autumn, thanks to the weakening of the central Adriatic gyre, and was directed only southwards or toward the Ionian Sea.

Connectivity patterns varied also from year to year (Table S2, Supporting Information). For instance, the weak connection between RA (northern Adriatic Sea) and FG (central Adriatic Sea) is the result of a unique connection event occurred in 2007. Also the connection between FG and LE (southern Adriatic Sea) allowed the exchange of individuals only in 2003 and 2007. Other connections, albeit subject to some interannual variability, allowed larval dispersal across locations in most years. The central Adriatic population sample (FG) showed the lowest retention (between 0.001% and 0.145%) and almost no connection with the other sites.

Discussion

The results of the molecular analysis indicate significant genetic differentiation of *Carcinus aestuarii*. Pairwise F_{ST}, AMOVA and STRUCTURE analyses concordantly identify the population from Sardinia (CA) as the most differentiated, in agreement with mitochondrial DNA sequencing (Marino *et al.* 2011). The use of microsatellites allowed the identification of weak, yet significant, differences also at a smaller geographic scale, which could not be detected by previous analyses: GENELAND identified three groups within the Adriatic–Ionian seas, whose differentiation was further supported by AMOVA. The first group includes the population samples from the northern Adriatic basin (MA, VE, GO and RA), the second contains that from the central Adriatic (FG), and the last one comprises those from southern Adriatic (LE) and Ionian (TA) sites.

Genetic homogeneity between Adriatic and Ionian populations has been demonstrated in several marine species, including *Atherina boyeri* (Congiu *et al.* 2002; Astolfi *et al.* 2005), *Sprattus sprattus* (Debes *et al.* 2008) and

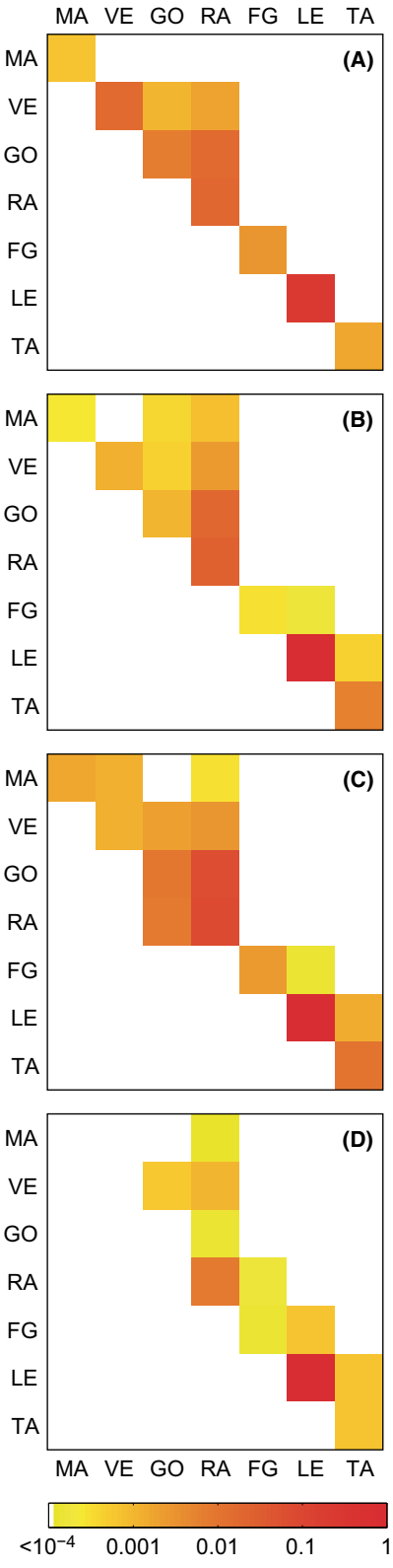

Fig. 4 Seasonal variability in oceanic connectivity among Adriatic and Ionian locations estimated by Lagrangian simulation. (A) September, (B) October, (C) November and (D) December. See Table 1 for location codes.

Paracentrotus lividus (Maltagliati *et al.* 2010). This pattern can be explained by historical factors, considering the recent colonization of the Adriatic Sea after the last glaciation maximum, assuming that Adriatic populations originated from the adjacent Ionian Sea (Astolfi *et al.* 2005; Pujolar *et al.* 2010; Marino *et al.* 2011). Alternatively, genetic homogeneity may be explained by contemporary gene flow, if a constant and significant coastal marine current connects the two areas, promoting larval exchange. This latter hypothesis is supported by the results of our CPBM simulations, showing that about 0.02% of the larvae released in the southern Adriatic can reach the Ionian Sea despite a waterway distance of almost 300 km. It is also in accordance with data obtained from surface drifter deployments in the Mediterranean Sea (MedSVP Program) and Lagrangian simulations performed in the same area to describe larval dispersal of *Diplodus sargus* (Pujolar *et al.* 2013). According to our simulations, larvae released from LE (southern Adriatic Sea) represent a significant proportion of the relevant sink site (TA, Ionian Sea), because of the concomitantly low retention at this latter site.

The subtle genetic differentiation observed among Adriatic population samples of *C. aestuarii* was previously undetected and not expected on the basis of the lack of genetic structure found, at a similar geographic scale, along the Iberian coast in the Atlantic sister species *C. maenas* (Domingues *et al.* 2010). Some degree of heterogeneity had been documented in *C. aestuarii* at the micro-geographic scale of the Venice Lagoon (Marino *et al.* 2010), but could be highlighted only by differentiation tests and was accompanied by nonsignificant F_{ST} values. In fact, when genetic differences are so subtle, the challenge is to discriminate between minor but real population structure and artefacts due to noise related to sampling errors (Wirth & Bernatchez 2001). Unfortunately, we cannot exclude that temporal variation has contributed to produce the clusters that we identified, as our sampling design did not include temporal replicates. This aspect is certainly worth further investigation; however, the results of the Lagrangian simulations provide an independent support for the existence of weak but significant geographic differentiation, apparently reflecting an oceanographic subdivision of the Adriatic Sea into three subbasins. This suggests that ocean circulation has an active role in determining spatial patterns of genetic differentiation in *C. aestuarii* populations of the Adriatic Sea, allowing the exchange of larvae through permanent connections (such as those linking north Adriatic sites) and ephemeral connections, such as those connecting the central Adriatic with northern and southern locations. This result is further supported by the MIGRATE-n analysis, showing that the best scenario to explain observed data is the one assuming a southward migration (in accordance with the general circulation of the basin and the directionality of exchange indicated by CPBM outputs), which outperformed a model envisaging a complete isolation among sites. The relevant role of contemporary factors in shaping the genetic differentiation in the Adriatic Sea is also supported by the lack of isolation by distance in this basin and by the absence of differences in genetic variability among samples. In fact, isolation by distance would be expected in case of a northward colonization after the Adriatic flooding and differences in genetic variability would be expected at the northern edge of the distribution in case of isolation and colonization involving small groups of dispersers (Hewitt 1996).

Genetic differentiation between the northern–central and the southern part of the Adriatic basin has been sporadically reported for pelagic and demersal species such as *Engraulis encrasicolus* (Bembo *et al.* 1996; Borsa 2002), *Scomber scombrus* (Zardoya *et al.* 2004; Papetti *et al.* 2013) and *Mullus barbatus* (Garoia *et al.* 2004). However, to our knowledge, this is the first study reporting a significant differentiation reflecting the oceanographic subdivision of the basin into three regions and providing a clear link between patterns of genetic differentiation and current-mediated gene flow. Considering that the Adriatic Sea is one of the most exploited basins in the Mediterranean and has been historically characterized by an intense fishery (Barausse *et al.* 2009), we believe that our approach combining genetic data with specific CPBM modelling provides a valuable methodological approach to investigate subtle differentiation patterns, generate hypotheses of connectivity by oceanographic models and refine stock definition in this area.

Acknowledgements

This project has received funding from the European Union's Seventh Framework Programme for Research, Technological Development and Demonstration under Grant Agreement No. 287844 (CoCoNET). We are thankful to Angelo Cau, Stefano Piraino and Fausto Tinti for providing us samples. Part of this work has been performed when IAMM was a PhD student in Evolutionary Biology at the University of Padova; IAMM is currently supported by a University of Padova post doc grant (CPDR123580/12).

References

Amos W, Hoffman JI, Frodsham A, Zhang L, Best S, Hill AVS (2007) Automated binning of microsatellite alleles: problems and solutions. *Molecular Ecology Notes*, **7**, 10–14.

Artegiani A, Bregant D, Paschini E, Pinardi N, Raicich F, Russo A (1997) The Adriatic sea general circulation. Part II: baroclinic circulation structure. *Journal of Physical Oceanography*, **27**, 1515–1532.

Astolfi L, Dupanloup I, Rossi R, Bisol PM, Faure E, Congiu L (2005) Mitochondrial variability of sand smelt *Atherina boyeri* populations from north Mediterranean coastal lagoons. *Marine Ecology Progress Series*, **297**, 233–243.

Barausse A, Duci A, Mazzoldi C, Artioli Y, Palmeri L (2009) Trophic network model of the Northern Adriatic Sea: analysis of an exploited and eutrophic ecosystem. *Estuarine Coastal and Shelf Science*, **83**, 577–590.

Beerli P, Felsenstein J (2001) Maximum likelihood estimation of a migration matrix and effective population sizes in n subpopulations by using a coalescent approach. *Proceedings of the National Academy of Sciences of the United States of America*, **98**, 4563–4568.

Beerli P, Palczewski M (2010) Unified framework to evaluate panmixia and migration direction among multiple sampling locations. *Genetics*, **185**, 313–326.

Behrens Yamada S, Hauck L (2001) Field identification of the European green crab species: *Carcinus maenas* and *Carcinus aestuarii*. *Journal of Shellfish Research*, **20**, 905–912.

Belkir K, Borsa P, Goudet J, Bonhomme F (2005) GENETIX v. 4.05, logiciel sous Windows pour la génétique des populations. Laboratoire Génome et Populations. CNRS UPR 9060, Université Montpellier II.

Bembo DG, Carvalho GR, Cingolani N, Pitcher TJ (1996) Electrophoretic analysis of stock structure in northern Mediterranean anchovies, *Engraulis encrasicolus*. *ICES Journal of Marine Science*, **53**, 115–128.

Bilodeau AL, Felder DL, Neigel JE (2005) Population structure at two geographic scales in the burrowing crustacean *Callichirus islagrande* (Decapoda, Thalassinidea): historical and contemporary barriers to planktonic dispersal. *Evolution*, **59**, 2125–2138.

Borsa P (2002) Allozyme, mitochondrial-DNA, and morphometric variability indicate cryptic species of anchovy (*Engraulis encrasicolus*). *Biological Journal of the Linnean Society*, **75**, 261–269.

Carson HS, López-Duarte PC, Rasmussen L, Wang D, Levin LA (2010) Reproductive timing alters population connectivity in marine metapopulations. *Current Biology*, **20**, 1926–1931.

Carvajal-Rodriguez A, de Uña-Alvarez J (2011) Assessing significance in high-throughput experiments by sequential goodness of fit and q-value estimation. *PLoS ONE*, **6**, e24700.

Chia FS, Buckland-Nicks J, Young CM (1984) Locomotion of marine invertebrate larvae: a review. *Canadian Journal of Zoology*, **62**, 1205–1222.

Congiu L, Rossi R, Colombo G (2002) Population analysis of the sand smelt *Atherina boyeri* (Teleostei Atherinidae), from Italian coastal lagoons by random amplified polymorphic DNA. *Marine Ecology Progress Series*, **229**, 279–289.

Cowen RK, Sponaugle S (2009) Larval dispersal and marine population connectivity. *Annual Review of Marine Science*, **1**, 443–466.

Dawson MN (2001) Phylogeography in coastal marine animals: a solution from California? *Journal of Biogeography*, **28**, 723–736.

Debes PV, Zachos FE, Hanel R (2008) Mitochondrial phylogeography of the European sprat (*Sprattus sprattus* L., Clupeidae) reveals isolated climatically vulnerable populations in the Mediterranean Sea and range expansion in the northeast Atlantic. *Molecular Ecology*, **17**, 3873–3888.

Di Franco A, Coppini G, Pujolar JM *et al.* (2012) Assessing dispersal patterns of fish propagules from an effective Mediterranean marine protected area. *PLoS ONE*, **7**, e52108.

Domingues CP, Creer S, Taylor MI, Queiroga H, Carvalho GR (2010) Genetic structure of *Carcinus maenas* within its native range: larval dispersal and oceanographic variability. *Marine Ecology Progress Series*, **410**, 111–123.

Dupont L, Ellien C, Viard F (2007) Limits to gene flow in the slipper limpet *Crepidula fornicata* as revealed by microsatellite data and a larval dispersal model. *Marine Ecology Progress Series*, **349**, 125–138.

Earl DA, vonHoldt BM (2012) STRUCTURE HARVESTER: a website and program for visualizing STRUCTURE output and implementing the Evanno method. *Conservation Genetics Resources*, **4**, 359–361.

Evanno G, Regnaut S, Goudet J (2005) Detecting the number of clusters of individuals using the software STRUCTURE: a simulation study. *Molecular Ecology*, **14**, 2611–2620.

Excoffier L, Lischer HEL (2010) Arlequin suite ver 3.5: a new series of programs to perform population genetics analyses under Linux and Windows. *Molecular Ecology Resources*, **10**, 564–567.

Excoffier L, Smouse PE, Quattro JM (1992) Analysis of molecular variance inferred from metric distances among DNA haplotypes: application to human mitochondrial DNA restriction data. *Genetics*, **131**, 479–491.

Falush D, Stephens M, Pritchard JK (2003) Inference of population structure using multilocus genotype data: linked loci and correlated allele frequencies. *Genetics*, **164**, 1567–1587.

Falush D, Stephens M, Pritchard JK (2007) Inference of population structure using multilocus genotype data: dominant markers and null alleles. *Molecular Ecology Notes*, **7**, 574–578.

Galarza JA, Carreras-Carbonell J, Macpherson E *et al.* (2009) The influence of oceanographic fronts and early-life-history traits on connectivity among littoral fish species. *Proceedings of the National Academy of Sciences of the United States of America*, **106**, 1473–1478.

Galindo HM, Olson DB, Palumbi SR (2006) Seascape genetics: a coupled oceanographic–genetic model predicts population structure of Caribbean corals. *Current Biology*, **16**, 1622–1626.

Galindo HM, Pfeiffer-Herbert AS, McManus MA, Chao Y, Chai F, Palumbi SR (2010) Seascape genetics along a steep cline: using genetic patterns to test predictions of marine larval dispersal. *Molecular Ecology*, **19**, 3692–3707.

Gallego A, North EW, Petitgas P (2007) Introduction: status and future of modelling physical–biological interactions during the early life of fishes. *Marine Ecology Progress Series*, **347**, 122–126.

Garoia F, Guarniero I, Ramšak A *et al.* (2004) Microsatellite DNA variation reveals high gene flow and panmictic populations in the Adriatic shared stocks of the European squid and cuttlefish (Cephalopoda). *Heredity*, **93**, 166–174.

Gilg MR, Hilbish TJ (2003) The geography of marine larval dispersal: coupling genetics with fine-scale physical oceanography. *Ecology*, **84**, 2989–2998.

Goudet J (2001) FSTAT, a program to estimate and test gene diversities and fixation indices (version 2.9.3). Available from http://www2.unil.ch/popgen/softwares/fstat.html.

Guarnieri A, Oddo P, Pastore M, Pinardi N, Ravaioli M (2010) The Adriatic basin forecasting system: new model and system development. In: *Coastal to Global Operational Oceanography: Achievements and Challenges. Proceeding of the Fifth International Conference on EuroGOOS, 20–22 May 2008, Exeter, UK* (eds Dahlin H, Bell MJ, Flemming NC, Petersson SE), pp. 184–190. EuroGOOS Publication, 28, BSH/EuroGOOS Office, Sweden.

Guillot G (2008) Inference of structure in subdivided populations at low levels of genetic differentiation. The correlated allele frequencies model revisited. *Bioinformatics*, **24**, 2222–2228.

Guillot G, Estoup A, Mortier F, Cosson JF (2005) A spatial statistical model for landscape genetics. *Genetics*, **170**, 1261–1280.

Hannah CG (2007) Future directions in modelling physical-biological interactions. *Marine Ecology Progress Series*, **347**, 301–306.

Hewitt GM (1996) Some genetic consequences of ice ages, and their role in divergence and speciation. *Biological Journal of the Linnean Society*, **58**, 247–276.

Hohenlohe PA (2004) Limits to gene flow in marine animals with planktonic larvae: models of *Littorina* species around Point Conception, California. *Biological Journal of the Linnean Society*, **82**, 169–187.

Hubisz M, Falush D, Stephens M, Pritchard J (2009) Inferring weak population structure with the assistance of sample group information. *Molecular Ecology Resources*, **9**, 1322–1332.

Jones DB, Jerry DR, McCormick MI, Bay LK (2010) The population genetic structure of a common tropical damselfish on the Great Barrier Reef and eastern Papua New Guinea. *Coral Reefs*, **29**, 455–467.

Kass RE, Raftery AE (1995) Bayes factors. *Journal of the American Statistical Association*, **90**, 773–795.

Kenchington EL, Patwary MU, Zouros E, Bird CJ (2006) Genetic differentiation in relation to marine landscape in a broadcast-spawning bivalve mollusc (*Placopecten magellanicus*). *Molecular Ecology*, **15**, 1781–1796.

Klassen G, Locke A (2007) *A Biological Synopsis of the European Green Crab, Carcinus maenas*. Canadian Manuscript report of Fisheries and Aquatic Sciences 2818. Fisheries and Oceans Canada, Gulf Fisheries Centre, Moncton, New Brunswick, pp. 82.

Knowlton N (2000) Molecular genetic analyses of species boundaries in the sea. *Hydrobiologia*, **420**, 73–90.

Maltagliati F, Di Giuseppe G, Barbieri M, Castelli A, Dini F (2010) Phylogeography and genetic structure of the edible sea urchin *Paracentrotus lividus* (Echinodermata: Echinoidea) inferred from the mitochondrial cytochrome b gene. *Biological Journal of Linnean Society*, **100**, 910–923.

Marino IAM, Barbisan F, Gennari M, Bisol PM, Zane L (2008) Isolation and characterization of microsatellite loci in the Mediterranean shore crab *Carcinus aestuarii* (Decapoda, Portunidae). *Molecular Ecology Resources*, **8**, 370–372.

Marino IAM, Barbisan F, Gennari M *et al.* (2010) Genetic heterogeneity in populations of the Mediterranean shore crab, *Carcinus aestuarii* (Decapoda, Portunidae), from the Venice Lagoon. *Estuarine Coastal and Shelf Science*, **87**, 135–144.

Marino IAM, Pujolar JM, Zane L (2011) Reconciling deep calibration and demographic history: bayesian inference of post glacial colonization patterns in *Carcinus aestuarii* (Nardo, 1847) and *C. maenas* (Linnaeus, 1758). *PLoS ONE*, **6**, e28567.

Marta-Almeida M, Dubert J, Peliz A, Queiroga H (2006) Influence of vertical migration pattern on retention of crab larvae in a seasonal upwelling system. *Marine Ecology Progress Series*, **307**, 1–19.

Mazzoldi C, Sambo A, Riginella E (2014) The Clodia database: a long time series of fishery data from the Adriatic Sea. *Scientific Data*, **1**, 140018.

Melià P, Schiavina M, Gatto M, Bonaventura L, Masina S, Casagrandi R (2013) Integrating field data into individual-based models of the migration of European eel larvae. *Marine Ecology Progress Series*, **487**, 135–149.

Morgan SG, Fisher JL, Miller SH, McAfee ST, Largier JL (2009) Nearshore retention and cross-shelf migration of larvae in a region of strong upwelling and recruitment limitation. *Ecology*, **90**, 3489–3502.

Mori M, Manconi R, Fanciulli G (1990) Notes on the reproductive biology of *Carcinus aestuarii* Nardo (Crustacea, Decapoda) from the lagoon of San Teodoro (Island of Sardinia, Italy). *Rivista di Idrobiologia*, **29**, 763–774.

Oddo P, Pinardi N, Zavatarelli M, Colucelli A (2006) The Adriatic basin forecasting system. *Acta Adriatica*, **47**, 169–184.

Orlić M, Gačić M, La Violette PE (1992) The currents and circulation of the Adriatic Sea. *Oceanologica Acta*, **15**, 109–124.

Palumbi SR (2003) Population genetics, demographic connectivity, and the design of marine reserves. *Ecological Applications*, **13**, S146–S158.

Papetti C, Di Franco A, Zane L *et al.* (2013) Single population and common natal origin for Adriatic *Scomber scombrus* stocks: evidence from an integrated approach. *ICES Journal of Marine Science*, **70**, 387–398.

Patwary MU, Kenchington EL, Bird CJ, Zouros E (1994) The use of random amplified polymorphic DNA (RAPD) markers in genetic studies of the sea scallop *Placopecten magellanicus* (Gmelin, 1791). *Journal of Shellfish Research*, **13**, 547–553.

Planes S (2002) Biogeography and larval dispersal inferred from population genetic analysis. In: *Ecology of Coral Reef Fishes: Recent Advances* (ed Sale PF), pp. 201–220. Academic Press, San Diego, California.

Pritchard JK, Stephens M, Donnelly P (2000) Inference of population structure using multilocus genotype data. *Genetics*, **155**, 945–959.

Pujolar JM, Marceta T, Saavedra C, Bressan M, Zane L (2010) Inferring the demographic history of the Adriatic *Flexopecten* complex. *Molecular Phylogenetics and Evolution*, **57**, 942–947.

Pujolar JM, Schiavina M, Di Franco A *et al.* (2013) Understanding the effectiveness of marine protected areas using genetic connectivity patterns and Lagrangian simulations. *Diversity and Distributions*, **19**, 1531–1542.

Queiroga H (1998) Vertical migration and selective tidal stream transport in the megalopa of the crab *Carcinus maenas*. *Hydrobiologia*, **375**(376), 137–149.

Queiroga H, Costlow JD, Moreira MH (1997) Vertical migration of the crab *Carcinus maenas* first zoea: implications for tidal stream transport. *Marine Ecology Progress Series*, **149**, 121–132.

R Development Core Team (2010) *R: A Language and Environment for Statistical Computing*. R Foundation for Statistical Computing, Vienna, Austria. ISBN 3-900051-07-0, Available from http://www.R-project.org.

Raymond M, Rousset F (1995) GENEPOP (version 1.2): population genetics software for exact tests and ecumenicism. *Journal of Heredity*, **86**, 248–249.

Reynolds J, Weir BS, Cockerham CC (1983) Estimation for the coancestry coefficient: basis for a short-term genetic distance. *Genetics*, **105**, 767–779.

deRivera CE, Hitchcock NG, Teck SJ, Steves BP, Hines AH, Ruiz GM (2007) Larval development rate predicts range

expansion of an introduced crab. *Marine Biology*, **150**, 1275–1288.

Rousset F (1997) Genetic differentiation and estimation of gene flow from F-statistics under isolation by distance. *Genetics*, **145**, 1219–1228.

Rousset F (2008) GENEPOP'007: a complete reimplementation of the GENEPOP software for Windows and Linux. *Molecular Ecology Resources*, **8**, 103–106.

Ryman N, Palm S (2006) POWSIM: a computer program for assessing statistical power when testing for genetic differentiation. *Molecular Ecology Notes*, **6**, 600–602.

Schunter C, Carreras-Carbonell J, Macpherson E *et al.* (2011) Matching genetics with oceanography: directional gene flow in a Mediterranean fish species. *Molecular Ecology*, **20**, 5167–5181.

Selkoe KA, Watson JR, White C *et al.* (2010) Taking the chaos out of genetic patchiness: seascape genetics reveals ecological and oceanographic drivers of genetic patterns in three temperate reef species. *Molecular Ecology*, **19**, 3708–3726.

Sherman CDH, Hunt A, Ayre DJ (2008) Is life history a barrier to dispersal? Contrasting patterns of genetic differentiation along an oceanographically complex coast. *Biological Journal of the Linnean Society*, **95**, 106–111.

Swearer SE, Shima JS, Hellberg ME *et al.* (2002) Evidence of self-recruitment in demersal marine populations. *Bulletin of Marine Science*, **70**(Suppl), 251–271.

Taylor MS, Hellberg ME (2003) Genetic evidence for local retention of pelagic larvae in a Caribbean reef fish. *Science*, **299**, 107–109.

Tepolt CK, Bagley MJ, Geller JB, Blum MJ (2006) Characterization of microsatellite loci in the European green crab (*Carcinus maenas*). *Molecular Ecology Notes*, **6**, 343–345.

Van Oosterhout C, Hutchinson WF, Wills DPM, Shipley P (2004) MICROCHECKER: software for identifying and correcting genotyping errors in microsatellite data. *Molecular Ecology Notes*, **4**, 535–538.

Waples RS (1998) Separating the wheat from the chaff: patterns of genetic differentiation in high gene flow species. *Journal of Heredity*, **89**, 438–450.

Waples RS, Gaggiotti O (2006) What is a population? An empirical evaluation of some genetic methods for identifying the number of gene pools and their degree of connectivity. *Molecular Ecology*, **15**, 1419–1439.

Ward RD, Woodwark M, Skibinski DOF (1994) A comparison of genetic diversity levels in marine, freshwater, and anadromous fishes. *Journal of Fish Biology*, **44**, 213–232.

Weir BS, Cockerham CC (1984) Estimating F-statistics for the analysis of population structure. *Evolution*, **38**, 1358–1370.

White C, Selkoe KA, Watson J, Siegel DA, Zacherl DC, Toonen RJ (2010) Ocean currents help explain population genetic structure. *Proceedings of the Royal Society of London, Series B*, **277**, 1685–1694.

Wirth T, Bernatchez L (2001) Genetic evidence against panmixia in the European eel. *Nature*, **409**, 1037–1040.

Zardoya R, Castilho R, Grande C *et al.* (2004) Differential population structuring of two closely related fish species, the mackerel (*Scomber scombrus*) and the chub mackerel (*Scomber japonicus*), in the Mediterranean Sea. *Molecular Ecology*, **13**, 1785–1798.